

# A mathematical model for predicting the carbon sequestration potential of ordinary portland cement (OPC) concrete



Adriana Souto-Martinez, Elizabeth A. Delesky, Kyle E.O. Foster, Wil V. Srubar III \*

Department of Civil, Environmental, and Architectural Engineering, Materials Science and Engineering Program, University of Colorado Boulder, ECOT 441 UCB 428, Boulder, CO 80309-0428, USA

## HIGHLIGHTS

- Total CO<sub>2</sub> sequestered by OPC concrete elements can be estimated (kg-CO<sub>2</sub>e).
- Variables include type of amount of cement, SCMs, exposure, time, and geometry.
- Low-C<sub>4</sub>AF cement, low SCM content, and high strengths increase sequesterable CO<sub>2</sub>.
- High SA/V ratios, indoor environments, and time enhance *in situ* CO<sub>2</sub> sequestration.

## ARTICLE INFO

### Article history:

Received 9 December 2016

Received in revised form 11 April 2017

Accepted 15 April 2017

Available online 2 May 2017

### Keywords:

Ordinary portland cement

Concrete

Carbonation

Carbon dioxide

Modeling

## ABSTRACT

A simple mathematical model that calculates the theoretical carbon sequestration potential of exposed ordinary portland cement (OPC) concrete is presented, validated, and implemented herein. OPC concrete sequesters non-trivial amounts of carbon dioxide (CO<sub>2</sub>) via carbonation – a chemical reaction between cement paste and atmospheric CO<sub>2</sub>. Formulated by the reaction chemistries of cement hydration and carbonation, the model accounts for cement type and content, exposure, time, and type and quantity of supplementary cementitious materials (SCMs). Once validated with data from literature, the model is implemented to investigate the effect of these factors and the influence of compressive strength and geometry, namely surface-area-to-volume (SA/V) ratio, on total carbon sequestration (kg CO<sub>2</sub>) of exposed concrete elements. Results demonstrate that (a) low tetracalcium aluminoferrite (C<sub>4</sub>AF) cements, (b) compressive strength, (c) high CO<sub>2</sub> exposure, (d) no SCMs, (e) time, (f) high SA/V ratios, and (g) indoor environments enhance the *in situ* carbon sequestration of exposed OPC concrete.

© 2017 Elsevier Ltd. All rights reserved.

## 1. Introduction

Buildings are responsible for approximately 40% of total energy consumption and 40% of carbon dioxide (CO<sub>2</sub>) emissions in the United States and Europe [1]. Achieving substantial reductions in these and other environmental impacts, such as acidification, eutrophication, and ozone depletion, involves identifying and quantifying impacts during all phases of a building's life cycle from material allocation, manufacture, construction, use, and disposal.

Several environmental assessment tools and methodologies, such as whole-building lifecycle assessment (WBLCA), have been developed for diverse purposes and users [2]. WBLCA has recently emerged as a methodological tool to help architects and structural engineers quantify and reduce potential lifecycle environmental impacts during the design phases of a building. Numerous exam-

ples of WBLCA implementation case studies can be found in the literature [3–8]. WBLCA can be applied, for instance, to identify environmental impact reduction strategies of high-impact materials or manufacturing processes. Researchers have elucidated, for example, that the manufacture of ordinary portland cement (OPC) currently accounts for 5–8% of anthropogenic global CO<sub>2</sub> emissions [9]. Numerous studies have since identified common best practices and strategies for reducing the environmental impacts of OPC concrete, which include minimizing total cement content and partially replacing cement with silica-rich supplementary cementitious materials (SCMs), such as fly ash, slag, silica fume, and metakaolin [10].

While the manufacture of OPC accounts for substantial CO<sub>2</sub> emissions due to limestone calcination, OPC pastes, mortars, and concretes also sequester small, but not trivial, amounts of CO<sub>2</sub> throughout their service life (a positive environmental benefit) via a chemical reaction process known as carbonation. However, only the negative impacts of OPC concrete are typically included

\* Corresponding author.

E-mail address: [wsrubar@colorado.edu](mailto:wsrubar@colorado.edu) (W.V. Srubar III).

when implementing lifecycle assessment (LCA) methodologies. The carbon sequestration potential of reinforced concrete is, at present, largely neglected in the environmental accounting. This omission is due, in part, to the complexity of predicting carbon sequestration potential and the lack of simple predictive models that can be implemented by practitioners and incorporated into LCA frameworks.

Previous research has largely addressed the mechanism of carbonation [11–15], and several analytical models have been developed to predict carbonation rates and depths in OPC concrete [16–22]. While these models emerged out of durability concerns of steel-reinforced concrete, a few recent studies have attempted to account for the amount of CO<sub>2</sub> sequestered during the service life of OPC concrete structures [23–30]. For example, Pade and Guimaraes [23] estimated CO<sub>2</sub> uptake due to carbonation over 100 years and compared it to the amount of CO<sub>2</sub> emitted during OPC manufacture. Collins [24] included CO<sub>2</sub> capture in a lifecycle assessment (LCA) of structural and crushed reinforced concrete. García-Segura et al. [26], studied the consequences of using blended cements in terms of enhanced durability and reductions in carbon sequestration. In addition, García-Segura et al. [31] and Yepes et al. [32] integrated estimates of sequestered carbon within a structural optimization framework to simultaneously consider cost and carbon emission in the design of prestressed concrete highway girders. Despite notable advances, however, these existing models exhibit complexities or limitations, including a limited capability to accommodate any cement or SCM type, which restricts their generalizability and implementation in practice.

The objective of this work was to formulate and implement a simple, yet robust, theoretical model for predicting the carbon sequestration potential of OPC concrete. The model, which is based on the hydration reaction and carbonation chemistries of OPC, accounts for variations in cement type, cement content, and cement replacement by SCMs. Only binary cements, namely OPC with the possible addition of one type of SCM, were considered. In formulating the model, average mineral contents for six different types of OPC, standardized by ASTM C150 [33], were linked to the carbon sequestration potential of the expected type and amount of hydration products. Anticipated reductions in carbonation potential due to the type and amount of SCMs were also incorporated. The resulting model directly calculates total anticipated carbon sequestration potential (kg CO<sub>2</sub>) from eight input variables, namely (1) total concrete volume, (2) total exposed concrete surface area, (3) cement type, (4) cement content per unit mass of concrete, (5) SCM type, (6) percent-replacement of cement with SCMs, (7) CO<sub>2</sub> exposure classification, and (8) time. The model is validated using data reported in the literature and implemented herein to demonstrate the effect of these variables, as well as the effect of concrete compressive strength and surface-area-to-volume (SA/V) ratio, on the carbon sequestration potential of exposed OPC concrete elements. The simplicity and generality of the model is preserved so that practicing architects and engineers can implement it in practice to maximize potential CO<sub>2</sub> sequestration during early stages of design.

## 2. Theoretical formulation and model implementation

### 2.1. Theoretical formulation

To calculate total sequesterable CO<sub>2</sub> for an exposed concrete element, first, the type of cement in the concrete mixture is mathematically linked to the theoretical type and amount of hydration reaction products, including calcium hydroxide (CH), also known as Portlandite, which is essential for the carbonation reaction. Next, the amount of CH is mathematically adjusted based on the

type and amount of SCMs present in the concrete mixture. Total sequesterable CO<sub>2</sub> per mass of carbonated cement paste is then calculated based on the stoichiometry of the carbonation reaction. Given the geometry of a concrete element (namely surface area and volume), length of time, and CO<sub>2</sub> exposure, total volume of carbonated concrete is calculated using a well-accepted predictive model for carbonation depth. Total volume of carbonated cement paste in the carbonated concrete is estimated using the known cement content per unit volume of concrete (kg/m<sup>3</sup>), which is obtainable from concrete mixture proportions. From these calculations, total sequesterable CO<sub>2</sub> (kg CO<sub>2</sub>) for a specific concrete element can be computed. Explicit mathematical details of the model formulation are presented in the following sections.

#### 2.1.1. Cement mineral content

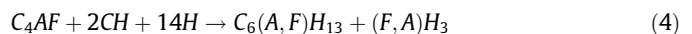
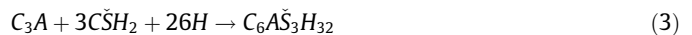
Table 1 lists the average chemical composition and mineral content for the main classifications of OPC as specified by ASTM C150 and White cement [33]. Primary oxides present in OPC, including silicon dioxide (S), aluminum oxide (A), ferric oxide (F), calcium oxide (C), magnesium oxide (M), sulfur trioxide (Š), and sodium oxide (N), comprise four main cement minerals, including tricalcium silicate (C<sub>3</sub>S), dicalcium silicate (C<sub>2</sub>S), tricalcium aluminate (C<sub>3</sub>A) and tetracalcium aluminoferrite (C<sub>4</sub>AF). Tailored mineral compositions enhance desired properties in the fresh- and hardened states, such as early strength, durability, or aesthetics in the case of White cement.

#### 2.1.2. Cement hydration reactions

The primary hydration reactions of tricalcium silicate (C<sub>3</sub>S) and dicalcium silicate (C<sub>2</sub>S) with water (H) produce both a calcium silicate hydrate (C<sub>3</sub>S<sub>2</sub>H<sub>8</sub>) phase and CH as follows:



The primary hydration reactions of other cement minerals, namely tricalcium aluminate (C<sub>3</sub>A) and tetracalcium aluminoferrite (C<sub>4</sub>AF) yields:



where, in cement chemistry notation, CŠH<sub>2</sub> is gypsum, C<sub>6</sub>ĀŠ<sub>3</sub>H<sub>32</sub> is ettringite, C<sub>6</sub>(A,F)H<sub>13</sub> is calcium aluminoferrite hydrate and (F,A)H<sub>3</sub> is aluminoferrite hydrate, respectively.

#### 2.1.3. Pozzolanic reaction

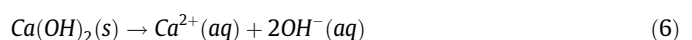
The addition of siliceous SCMs effectively reduces the carbon sequestration potential of hydrated portland cement by reacting with available CH to produce CSH according to the following reaction:



Therefore, the total amount of available CH in a given concrete mixture must be mathematically adjusted based on the type and amount of SCM in the concrete mixture (see Section 2.1.5).

#### 2.1.4. Carbonation reaction

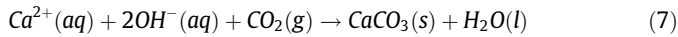
The process of carbonation is a chemical reaction that occurs primarily between readily available CH and atmospheric CO<sub>2</sub> that precipitates calcite, the most stable polymorph of calcium carbonate, CaCO<sub>3</sub>. In conventional chemistry notation, the reactions are as follows:



**Table 1**

Average chemical and mineral composition of cement types by weight according to ASTM C150 [33]. Oxides and minerals are presented in cement chemistry notation.

Cement type	Average oxide composition (%)								Average mineral (Bogue) composition (%)				
	S (SiO <sub>2</sub> )	A (Al <sub>2</sub> O <sub>3</sub> )	F (Fe <sub>2</sub> O <sub>3</sub> )	C (CaO)	M (MgO)	Š (SO <sub>3</sub> )	N (Na <sub>2</sub> O)	Other	C <sub>3</sub> S	C <sub>2</sub> S	C <sub>3</sub> A	C <sub>4</sub> AF	Other
I	20.5	5.4	2.6	63.9	2.1	3.0	0.61	1.9	54	18	10	8	10
II	21.2	4.6	3.5	63.8	2.1	2.7	0.51	1.6	55	19	6	11	9
III	20.6	4.9	2.8	63.4	2.2	3.5	0.56	2.0	55	17	9	8	11
IV	22.2	4.6	5.0	62.5	1.9	2.2	0.36	1.2	42	32	4	15	7
V	21.9	3.9	4.2	63.8	2.2	2.3	0.48	1.2	54	22	4	13	7
White	22.7	4.1	0.3	66.7	0.9	2.7	0.18	2.4	63	18	10	1	8



While trace amounts of magnesium and sodium are present in cement, the precipitation of other alkali and alkaline carbonate salts via similar carbonation reactions is not thermodynamically favored.

This formulation assumes, albeit conservatively, that only available CH participates in the carbon sequestration. Many research studies have highlighted the role of calcium silicate hydrate (CSH) in the carbonation process [34]. In addition, the ferritic phases in cement paste (e.g., Aft, AFm) have been shown to carbonate [35]. However, to preserve simplicity, these carbonation reactions have not been included in the mathematical formulation. The formulation also assumes that no carbonation occurs after CH depletion. However, further carbonation is likely, due to the existence of calcium-containing compounds (i.e., CSH) formed via pozzolanic reactions with siliceous SCMs. The assumption that only available CH participates in carbon sequestration, however, is conservative, in that the model will not produce overestimations of sequesterable carbon, but rather err on the side of underprediction.

A negative impact of carbonation is that CO<sub>2</sub> gas, which initially dissolves in water to form carbonic acid, H<sub>2</sub>CO<sub>3</sub>, can subsequently react with alkalis in the pore solution (e.g., Ca<sup>2+</sup>). The depletion of hydroxide ions (OH<sup>-</sup>) from the pore solution chemistry effectively lowers the pH of the pore solution from approximately 12.5 to 9.0. This reduction can destabilize the protective passive oxide layer that initially forms on the surface of mild steel reinforcement. Destabilization of the passive layer can lead to reinforcement corrosion in the presence of sufficient oxygen and water. Therefore, sufficient cover depth is required to protect steel reinforcement, especially in severe exposure conditions. Alternative reinforcement strategies, such as the use of epoxy-coated rebar or glass fiber-reinforced polymer (GFRP) rebar, can increase the service-life of reinforced OPC concrete that may be prone to chemical deterioration via carbonation.

#### 2.1.5. Carbon sequestration potential of hydrated cement paste

From these equations, the theoretical amount of sequesterable CO<sub>2</sub> via the formation of calcium carbonate in the hydrated cement paste on a per mass basis can be computed according to the following equation:

$$C_m = \alpha - \beta \cdot y \quad (8)$$

where carbon sequestration potential,  $C_m$ , is defined as the total mass percentage of sequesterable CO<sub>2</sub> per kg of carbonated cement paste (kg CO<sub>2</sub>/kg cement) in the concrete and  $y$  is the percent replacement (by mass of cement) by SCMs in decimal form. Table 2 lists values for the coefficient  $\alpha$ , which accounts for variation in cement type. Assuming a theoretical 100% hydration of cement minerals,  $\phi_h = 1.0$ , the  $\alpha$  coefficient reported in Table 1 was obtained by the following equation:

$$\alpha = \phi_h MW_{CH} \left( \frac{3}{2} \cdot \frac{B_{C_3S}}{MW_{C_3S}} + \frac{1}{2} \cdot \frac{B_{C_2S}}{MW_{C_2S}} - \frac{2}{1} \cdot \frac{B_{C_4AF}}{MW_{C_4AF}} \right) \quad (9)$$

where  $B_{C_3S}$ ,  $B_{C_2S}$ , and  $B_{C_4AF}$  are the Bogue composition (%) of C<sub>3</sub>S, C<sub>2</sub>S, and C<sub>4</sub>AF, respectively, and  $MW_{C_3S}$ ,  $MW_{C_2S}$ ,  $MW_{C_4AF}$ , and  $MW_{CH}$  are the molecular weights of C<sub>3</sub>S (228.314 g/mol), C<sub>2</sub>S (172.237 g/mol), C<sub>4</sub>AF (485.955 g/mol), and CH (74.09 g/mol). Multipliers (3/2), (1/2), and (2) are stoichiometric ratios of CH produced or consumed by C<sub>3</sub>S, C<sub>2</sub>S, and C<sub>4</sub>AF, respectively, in the hydration reactions presented in Eqs. (1), (2), and (4). The relative magnitudes of the  $\alpha$  parameter are quantitative measures of the amount of readily available CH that is produced by the hydration reactions.

To validate these predictions, similar calculations were obtained for total theoretical grams (g) of CH produced per gram of cement assuming 100% hydration. The results yield values of 0.28, 0.28, 0.28, 0.23, and 0.27 kg CH per kg cement for cement Types I–V, respectively, which align well with the empirical and theoretical predictions of CH content as a function of hydration degree reported in [36].

The coefficient  $\beta$  accounts for the type and amount of SCMs. If the total silica content of the actual SCM is known, or can be obtained via laboratory analysis prior to mixture proportioning, the coefficient  $\beta$  can be computed according to the general equation:

$$\beta = 1.1 \cdot \sigma \quad (10)$$

where  $\sigma$  is the weight percent (%) of silicon dioxide (SiO<sub>2</sub>) in the SCM in decimal form. The scalar of 1.1 was derived by dividing the molar ratio of calcium hydroxide to silica shown in Eq. (6) (3/2) by the molecular weight of silicon dioxide (60.083 g/mol) and multiplied by the molecular weight of CO<sub>2</sub> (44.01 g/mol), which yields a final scale factor of  $1.09873 \approx 1.1$ . If the total silica content is neither known nor obtainable via chemical analysis, average silica contents for common types of SCM are listed in Table 2. However, it is cautioned that the utilization of average silica contents listed in Table 2 will impart uncertainty in the modeling prediction.

#### 2.1.6. Carbonation depth

Accurately predicting carbonation depth after a period of prolonged exposure is difficult because the process is complex. The depth of the carbonation front is affected by moisture, temperature, CO<sub>2</sub> concentration, time, and, as discussed, type and amount of cement and SCMs, which dictates the availability of reactive CH.

Despite these challenges, an empirical model for predicting the carbonation depth,  $x$  (mm), has been proposed by the Portuguese National Laboratory [17] and used by previous researchers:

$$x = \sqrt{\left( \frac{2 \cdot c \cdot t}{R} \right)} \cdot \left[ \sqrt{k_0 k_1 k_2} \left( \frac{1}{t} \right)^n \right] \quad (11)$$

where  $c$  is the environmental CO<sub>2</sub> concentration (kg/m<sup>3</sup>) (Note: 1 kg/m<sup>3</sup> CO<sub>2</sub> = 516 ppb),  $t$  is exposure time (years),  $k_0$  is equal to 3.0,  $k_2$  is equal to 1.0 for standard curing, and  $R$  is the carbonation resistance coefficient (kg year/m<sup>5</sup>) that is calculated for Type I and Type II cement according to:

$$R = 0.0016 \cdot f_c^{3.106} \quad (12)$$

**Table 2**

Carbon sequestration potential coefficients per cement type and SCM.

Cement Type	$\alpha$	Supplementary Cementitious Material (SCM)	Average $\sigma$ % SiO <sub>2</sub>	$\beta$
Type I	0.165	Fly Ash (Class F)	50%	0.55
Type II	0.163	Fly Ash (Class C)	25%	0.27
Type III	0.166	Slag	35%	0.38
Type IV	0.135	Silica Fume	90%	0.99
Type V	0.161	Metakaolin	50%	0.55
White	0.203			

and for Types III–V and White cement according to:

$$R = 0.0018 \cdot f_c^{2.862} \quad (13)$$

where  $f_c$  is the compressive strength (MPa). The factors  $k_1$  and  $n$ , shown in Table 3, are dependent upon exposure classifications as outlined below in Table 4.

### 2.1.7. Total carbonated volume

To calculate total carbonated volume, first, the type of cement (Type I–V/White), design compressive strength, and mixture proportions, namely the total mass (kg) per unit volume (m<sup>3</sup>) of concrete, of concrete must be known, as well as the initial exposed surface area,  $SA$ , and total volume of all structural and non-structural exposed concrete members. Exposed concrete includes concrete elements without coatings or paints that may inhibit ingress of CO<sub>2</sub>.

The total carbonated volume at any finite point in time can be calculated by multiplying the total carbonation depth,  $x$ , computed according to Eq. (11), by the total surface area of exposed concrete members:

$$V_c = SA \cdot x \quad (14)$$

with the limitation that the total carbonated concrete volume,  $V_c$ , must be less than or equal to the total volume of OPC concrete,  $V$ . The theoretical limit of sequesterable CO<sub>2</sub> of a given volume of concrete after an infinite amount of time can be calculated by assuming  $V_c = V$ .

### 2.1.8. Total mass of sequestered CO<sub>2</sub>

The total mass of sequesterable CO<sub>2</sub>,  $C_s$  (kg CO<sub>2</sub>), can be calculated by multiplying the total mass of carbonated cement paste by the carbon sequestration potential,  $C_m$ , calculated according to Eq. (8):

$$C_s = \phi_c C_m \cdot [V_c \cdot m] \quad (15)$$

where  $\phi_c$  is the degree of carbonation,  $m$  is the total mass of cement per unit volume of concrete (kg/m<sup>3</sup>) obtained from the concrete batch mixture proportions, and the quantity in brackets is equal to the total mass of carbonated cement paste. While a theoretical 100% degree of carbonation,  $\phi_c = 1.0$ , is assumed herein for model implementation and demonstration purposes, actual degrees of carbonation ranging from 0.40 to 0.72 have been experimentally obtained by previous researchers [37–41]. Lower degrees of carbonation are more conservative, which will result in lower estimates of sequestered CO<sub>2</sub>.

**Table 3**Parameter values for  $k_1$  and  $n$  based on exposure classification [17].

Parameter	XC1	XC2	XC3	XC4
$k_1$	1.0	0.20	0.77	0.41
$n$	0	0.183	0.02	0.085

**Table 4**

Carbonation environmental exposure classifications [17].

Class	Environment	Examples
XC1	Dry or permanently humid	Reinforced concrete inside buildings or structures, except areas of high humidity; Reinforced concrete permanently under non-aggressive water.
XC2	Humid, rarely dry	Reinforced concrete under non-aggressive soil; Reinforced concrete subjected to long periods of contact with non-aggressive water.
XC3	Moderately humid	Outer surfaces of reinforced concrete sheltered from wind-driven rain; Reinforced concrete inside structures with moderate to high air humidity.
XC4	Cyclically humid and dry	Reinforced concrete exposed to wetting/drying cycles; Outer surfaces of reinforced concrete exposed to rain or outside the scope of XC2.

## 2.2. Model validation

Experimental data related to carbonation exist in the literature, yet the majority of studies focus on validation of predictive models for carbonation-induced corrosion. As previously discussed, only a few studies have used carbonation data to predict total sequestered CO<sub>2</sub> (kg CO<sub>2</sub>) by concrete elements *in situ*. Some studies present specific examples used herein for comparison. Table 5 shows comparative values reported by those authors and those predicted by the model, along with the modeling parameters and assumptions (if any) that used for validation.

The results substantiate that predicted values for total carbon sequestration of concrete elements align well with those reported by other studies. For example, according to results obtained by García-Segura et al. [26], a  $0.3 \times 0.3 \times 3$  m ( $SA/V = 14$  m<sup>−1</sup>) Type I, 25 MPa concrete column sequesters up to 16.4 kg CO<sub>2</sub> after 100 years of exposure. The mathematical model presented herein predicts that the same Type I, 25 MPa concrete column with an identical geometry would theoretically sequester a maximum of approximately 17.0 kg CO<sub>2</sub>, a difference of 3.7%. Similar results were obtained for the other case studies, establishing that the proposed generalized mathematical approach is a valid estimate of theoretical carbon sequestration potential in OPC and blended OPC cement concretes.

## 2.3. Model implementation

The model formulated in Section 2.1 was implemented to investigate the effect of cement type, cement content, and time, as well as the type and amount of SCMs on carbon sequestration potential of exposed concrete elements. In addition, the influence of (a) design compressive strength, (b) exposure classification, and (c) structural geometry on the carbon sequestration potential of reinforced concrete elements was investigated herein.

### 2.3.1. Influence of design compressive strength

To elucidate the effects of concrete compressive strength, sample concrete mixtures of varying 28-day compressive strengths were designed according to the Portland Cement Association con-



**Table 5**  
OPC concrete element case studies and parameters used for model validation [25,26,28–30].

Sample	Cement Type	Cement Content (kg/m <sup>3</sup> )	Compressive Strength (MPa)	SCM Type	SCM Quantity (%)	$\phi_c$ (%)	Surface Area (m <sup>2</sup> )	Volume (m <sup>3</sup> )	Exposure Class	CO <sub>2</sub> (ppm)	Time (years)	Reported (kg CO <sub>2</sub> )	Model prediction (kg CO <sub>2</sub> )	Reference
1	Type I*	373	>35	Fly Ash (Class C)	36	0.75	2.21	0.221	Outdoor Exposed	300	70	1.8	1.3	Pomer & Pade (2006)
2	Type I*	480	>35	–	–	0.75	2.00	0.017	Outdoor Exposed	300	50	0.9	1.0	Pomer & Pade (2006)
3	Type I*	349–463	24–35	Fly Ash (Class C)	12.9–14.9	0.75–1.0	14,400–17,800	11.743	Outdoor/Indoor	300–800	20	91.5	50.2–110.6	Lee, et al. (2012)
4	Type I	250	25	–	–	0.75–1.0	3.6	0.27	Outdoor/Indoor	300–800	100	16.4	7.0–16.99	García-Segura, et al. (2013)
5	Type II	250	25	Fly Ash (Class C)	20	0.75–1.0	3.6	0.27	Outdoor/Indoor	300–800	100	11.4	2.35–11.63	García-Segura, et al. (2013)
6	Type II	360	30	–	–	0.75	9.6	NS	Indoor	800	50	36.4*	27.8	Lagerblad (2006)
7	Type I	277	NS	–	–	0.35	NS	NS	Indoor	800	100	6.1	5.8	Nilsson & Fridh (2011)

\* Denotes assumed modeling parameter or calculated result from reference studies.

crete mixture design methodology [42]. In order to calculate cement content, each concrete mixture was initially designed using a Type I ASTM C 150 cement with a relative density of 3.15, maximum coarse aggregate size of 2 cm with an oven-dry relative density of 2.68 (ASTM C 33), natural sand with an oven-dry relative density of 2.64 (ASTM C 33), an air-entraining mixture of wood-resin type (ASTM C 260), and 7% air content. The resulting sample mixtures are shown below in Table 6.

### 2.3.2. Influence of environmental exposure

CO<sub>2</sub> concentration depends on exposure classification. An XC1 exposure is used, for example, for cases where reinforced concrete is located inside buildings or structures, where the CO<sub>2</sub> concentration is high in comparison to a XC4 exposure, where outer surfaces of concrete elements are exposed to the outdoors. On average, indoor concentrations are approximately 700 ppm above normal outdoor CO<sub>2</sub> concentrations, which range between 300 and 500 ppm [43]. For the purposes of this study, the assumed placement of elements (indoor vs. outdoor) is linked to XC1 and XC4 exposure classification and to CO<sub>2</sub> concentrations of 800 ppm ( $1.55 \times 10^{-3}$  kg/m<sup>3</sup>) and 300 ppm ( $0.581 \times 10^{-3}$  kg/m<sup>3</sup>), respectively.

### 2.3.3. Influence of structural geometry

Given that the carbonation process is a surface-dominated, rate-dependent phenomenon, the total amount of sequesterable CO<sub>2</sub> per unit time is related to the carbonation depth and total exposed surface area in direct contact with air or water. For this reason, the geometry, namely the surface area, SA, and total volume, V, of concrete elements will directly influence total CO<sub>2</sub> sequestration. To investigate the effect of surface-area-to-volume (SA/V) ratio on CO<sub>2</sub> sequestration potential, several cross-sectional geometries of concrete columns were considered. The cross-sectional area (0.25 m<sup>2</sup>), length (3 m), and volume (0.75 m<sup>3</sup>) of each column were held constant. Table 7 illustrates the shape, cross-sectional dimensions, total surface area, and SA/V ratios of the concrete columns considered herein.

## 3. Results and discussion

### 3.1. Effect of cement type

Fig. 1 shows the effect of cement type on carbon sequestration potential of a  $0.5 \times 0.5 \times 3$  m ( $SA/V = 8 \text{ m}^{-1}$ ) concrete column (Cross-Section #2, Table 7) for all types of cement after 25, 50, 75, 100, 125 and 150 years in both an indoor environment (XC1) with a high concentration (800 ppm,  $1.55 \times 10^{-3}$  kg/m<sup>3</sup>) of CO<sub>2</sub> and an outdoor environment (XC4) with low concentration (300 ppm,  $0.581 \times 10^{-3}$  kg/m<sup>3</sup>) of CO<sub>2</sub>. A compressive strength of 40 MPa was assumed, and no SCMs were added to isolate the effect of cement type on carbon sequestration potential.

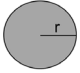

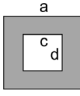
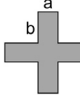

Expectedly, the total amount of sequestered CO<sub>2</sub> increases with both exposure time and favorable exposure conditions. For example, the Type I cement concrete column exhibits a 145% increase in sequesterable CO<sub>2</sub> between 25 and 150 years in a XC1 (high-CO<sub>2</sub>) environment. A 289% increase is observed for the same Type I cement concrete column in a XC1 versus XC4 (low-CO<sub>2</sub>) environment after 150 years of exposure. All cement types exhibit similar time- and exposure-dependent behaviors.

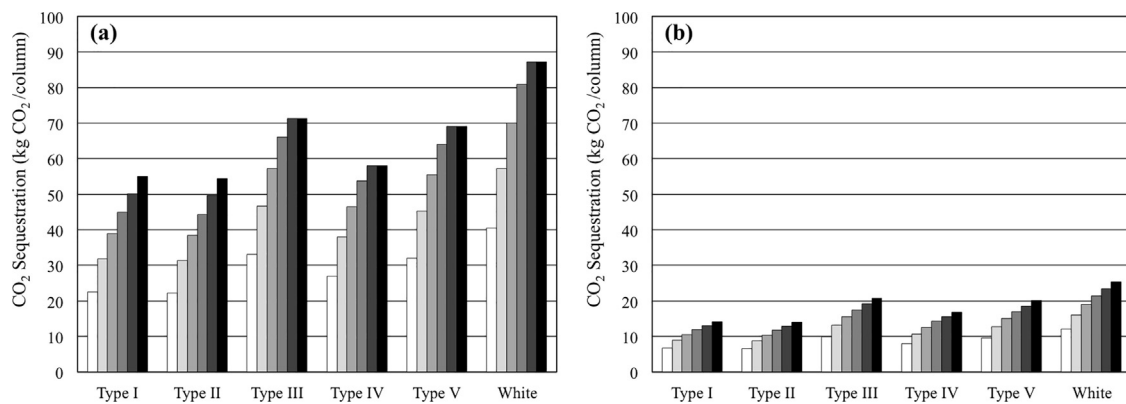
White cement concrete consistently sequesters more CO<sub>2</sub> than other cement types due to its inherently low C<sub>4</sub>AF mineral composition. According to Eq. (4), hydration of C<sub>4</sub>AF consumes CH, thus, low C<sub>4</sub>AF would result in more CH available for CO<sub>2</sub> sequestration. Similarly, the Type III cement concrete exhibits the second-highest CO<sub>2</sub> sequestration potential, due to its lower

**Table 6**Sample mixture proportions (kg/m<sup>3</sup>) for concretes of varying compressive strengths.

Concrete Mixture Constituents	Concrete Design Compressive Strength				
	15 MPa	25 MPa	30 MPa	40 MPa	45 MPa
Cement	281	381	451	572	641
Water	102	106	110	115	118
Coarse Aggregate	1013	1013	1013	1013	1013
Fine Aggregate	866	1310	715	698	547

**Table 7**Column geometries considered in analyzing the effect of SA/V on carbon sequestration potential. Each column had a fixed cross-sectional area (0.25 m<sup>2</sup>), length (3 m), and volume (0.75 m<sup>3</sup>).

Cross-Section	Geometry	Dimensions (m)	Total Surface Area (m <sup>2</sup> )	SA/V Ratio (m <sup>-1</sup> )
1		r = 0.28	5.3	7.1
2		a = 0.5; b = 0.5	6.0	8.0
3		a = 0.6; b = 0.6; c = 0.33; d = 0.33	11.2	14.9
4		a = 0.14; b = 0.4	11.3	15.1
5		a = 0.1; b = 2.4	15.0	20.0

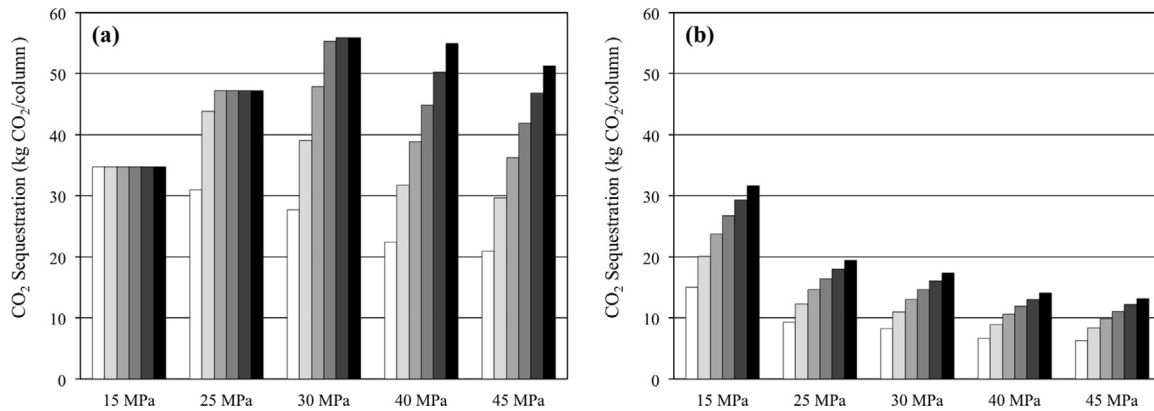
**Fig. 1.** Effect of cement type on carbon sequestration potential in (a) XC1 high-(800 ppm) and (b) XC4 low-concentration (300 ppm) CO<sub>2</sub> environments after 25 (○), 50 (●), 75 (●), 100 (●), 125 (●), and 150 (●) years of exposure for a 40 MPa concrete column (0.5 × 0.5 × 3 m, SA/V = 8 m<sup>-1</sup>).

C<sub>4</sub>AF content compared to Type I, II, IV, and V cements (Table 1). Type I and Type II cement concretes exhibit similar behaviors in both CO<sub>2</sub> environments. This behavior is anticipated due to similarities in both chemical composition and carbonation resistance of Type I and Type II cements.

The diminishing effect of total sequestered CO<sub>2</sub> with time is demonstrated by all cement types in both CO<sub>2</sub> environments. Type I and White cement concrete columns sequester 22.4 kg CO<sub>2</sub> and 40.5 kg CO<sub>2</sub>, respectively, for this application after the first 25 years of exposure in a XC1 high-concentration CO<sub>2</sub> environment. These columns only sequester an additional 32.5 kg CO<sub>2</sub> and 46.8 kg CO<sub>2</sub>, respectively, after 125 years of further exposure (150 years).

This reduction in the rate of CO<sub>2</sub> sequestration is attributable to the time-dependent decay in total carbonation depth (Eq. (11)).

Fig. 1a also demonstrates that the total volume of this particular concrete column can carbonize in its entirety while exposed in-service to a XC1 high CO<sub>2</sub> concentration environment. For example, Type III, IV, V and White cement concrete columns reach their maximum theoretical carbon sequestration potential after 125 years of exposure. The theoretical maximum for a Type IV cement, 40 MPa concrete column is 58 kg CO<sub>2</sub>, while, for a White cement, 40 MPa concrete column of identical volume, an additional 50% can be sequestered (87 kg total). These results demonstrate that reaching the theoretical carbon sequestration potential during



**Fig. 2.** Effect of compressive strength on the carbon sequestration potential in (a) XC1 high-(800 ppm) and (b) XC4 low-concentration (300 ppm)  $\text{CO}_2$  environments after 25 (○), 50 (●), 75 (●), 100 (●), 125 (●), and 150 (●) years of exposure for a Type I cement concrete column ( $0.5 \times 0.5 \times 3$  m,  $\text{SA}/\text{V} = 8 \text{ m}^{-1}$ ).

service depends not only on exposure conditions, but also on cement composition.

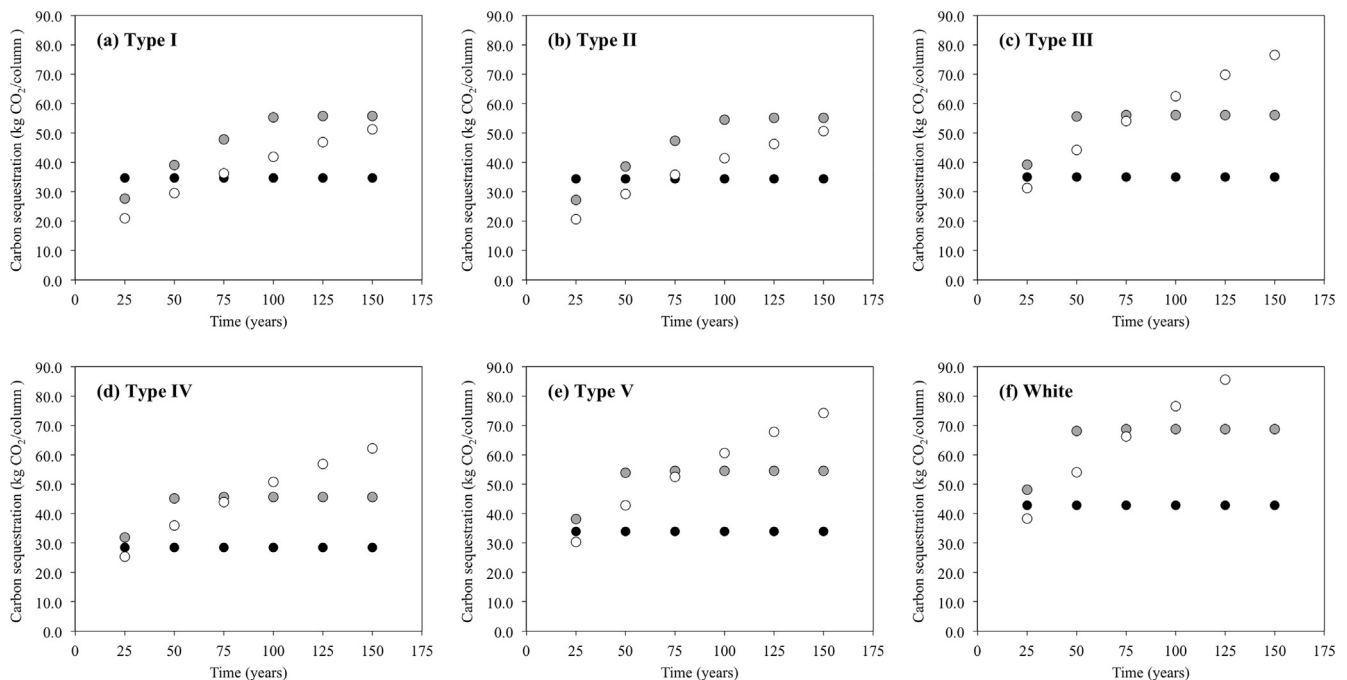
### 3.2. Effect of concrete compressive strength

Similar to the effects of cement type, compressive strength, which is highly governed by cement (and water) content, directly influences both in-service and total carbon sequestration potential. Fig. 2 illustrates the effect of design compressive strength on the carbon sequestration potential of Type I cement concrete mixtures (see Table 6) for a  $0.5 \times 0.5 \times 3$  m column ( $\text{SA}/\text{V} = 8 \text{ m}^{-1}$ ) after 25, 50, 75, 100, 125 and 150 years of exposure in both an indoor (XC1) a high-concentration (800 ppm) (Fig. 2a) and outdoor (XC4) low-concentration (300 ppm)  $\text{CO}_2$  environment (Fig. 2b).

Again, as anticipated, the theoretical sequesterable  $\text{CO}_2$ , in general, increases with time and with favorable exposure conditions for each concrete mixture. A Type I, 40 MPa concrete column, for example, exhibits a 145% increase in sequesterable  $\text{CO}_2$  between

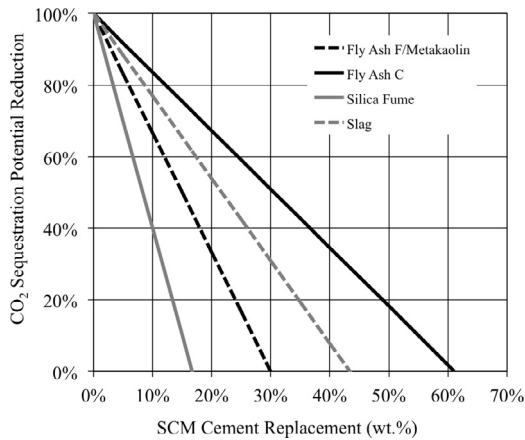
25 and 150 years in a XC1 environment (Fig. 2a). A 290% increase is observed for the same Type I, 40 MPa concrete column in a XC1 versus XC4 environment after 150 years of exposure. Similar time- and concentration-dependent behavior is exhibited by all mixture formulations except the Type I 15 MPa, 25 MPa, and 30 MPa concrete columns, which, as illustrated by the plateaus in the data (Fig. 2a), reach the theoretical carbon sequestration limit in a XC1 high-concentration  $\text{CO}_2$  environment after 25, 75, and 125 years of exposure, respectively.

Fig. 2b also demonstrates that, in general, an increase in compressive strength correlates to reductions in total sequesterable  $\text{CO}_2$  at early ages (25–50 years). This trend is also observable for the non-plateaued data for the 40 MPa and 50 MPa columns in Fig. 2a. However, the theoretical limit of total sequesterable  $\text{CO}_2$  is, in fact, maximized in high-compressive strength concretes as the total carbonated volume approaches the total concrete volume ( $V_c \rightarrow V$ ) as  $t \rightarrow \infty$ , which is suggested by the plateaued data in Fig. 2a for the 15 MPa, 25 MPa, and 30 MPa columns. Increased



**Fig. 3.** Effect of cement type, namely (a) Type I, (b) Type II, (c) Type III, (d) Type IV, (e) Type V, and (f) White, and time on the carbon sequestration potential of 15 MPa (●), 30 MPa (●), and 45 MPa (○) compressive strength concrete columns ( $0.5 \times 0.5 \times 3$  m,  $\text{SA}/\text{V} = 8 \text{ m}^{-1}$ ) in a high-concentration (800 ppm)  $\text{CO}_2$  environment.

compressive strengths require higher cement contents (see Table 6), thus increasing the theoretical potential for  $\text{CO}_2$  sequestration (Eq. (15)). However, the carbonation resistance factor,  $R$ , also increases with compressive strength (Eq. (12)). This increase is attributable to denser microstructures and lower overall gas and liquid permeabilities that result from high-strength concrete mixtures. In sum, the data show that lower compressive strengths, high  $\text{CO}_2$  exposure, and time increase the total sequesterable  $\text{CO}_2$

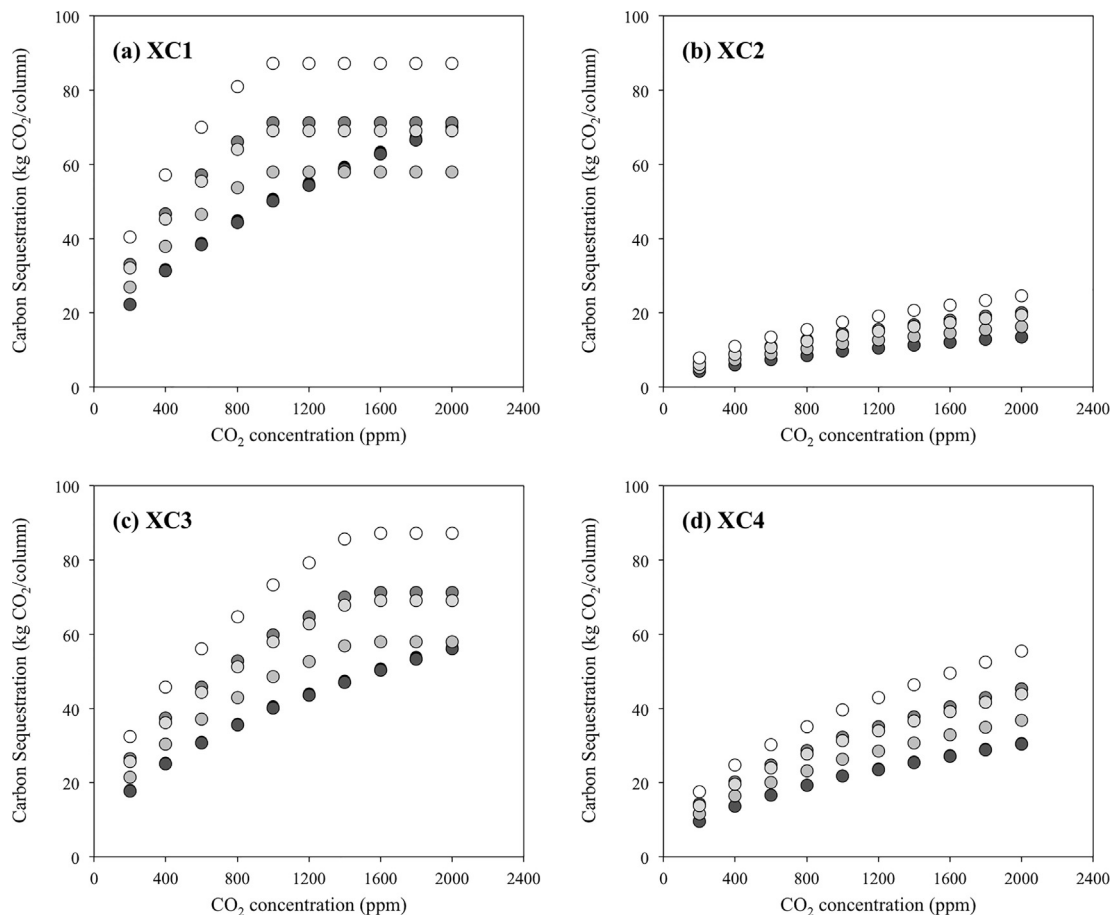


**Fig. 4.** Anticipated reductions in carbon sequestration potential,  $C_m$ , per SCM type and weight-percent cement replacement. Data shown are valid for all cement types (Type I–V, White).

at early ages. However, this time- and exposure-dependent reduction is overcome at later ages. To illustrate, a Type I 25 MPa concrete column sequesters 31.0 kg  $\text{CO}_2$ , while a Type I 45 MPa concrete sequesters 21.0 kg  $\text{CO}_2$  after 25 years in a XC1 high-concentration (800 ppm)  $\text{CO}_2$  environment. The theoretical carbon sequestration limits for the Type I 25 MPa and Type I 45 MPa concrete columns (as  $t \rightarrow \infty$ ), however, are 47.2 kg  $\text{CO}_2$  and 59.2 kg  $\text{CO}_2$  (data not shown), respectively.

While these data were specific for a Type I cement concrete, the effect of cement type, compressive strength, and time on carbon sequestration potential of a concrete column with equal dimensions in a XC1 high-concentration (800 ppm)  $\text{CO}_2$  environment is illustrated in Fig. 3.

These results show that more  $\text{CO}_2$  is sequestered (1) in lower-strength concretes at early ages, (2) in higher-strength concretes at later ages, and (3) in concretes with low- $C_4\text{AF}$  cements (i.e., Type III, Type V, White). For instance, after 25 years of exposure, a Type I, 15 MPa concrete column sequesters 66% more  $\text{CO}_2$  than a Type I, 45 MPa concrete column. After 150 years, however, the Type I, 45 MPa concrete sequesters 47% more  $\text{CO}_2$  than the Type I, 15 MPa concrete column (Fig. 3a). Furthermore, a low- $C_4\text{AF}$  White cement 45 MPa concrete, sequesters 83% more  $\text{CO}_2$  than the Type I, 45 MPa concrete after 150 years. All concrete specimens demonstrate that approximately 40% of all carbon sequestration occurs within the first 25 years of exposure. Additionally, for low-strength concrete columns with, hence, a lower carbonation resistance factor,  $R$ , the theoretical maximum carbonation is reached after 50 years of exposure for this column geometry, as noted by the 15 MPa concrete plateau effect in Fig. 3a–f.



**Fig. 5.** Effect of  $\text{CO}_2$  concentration and exposure environment, namely (a) XC1, (b) XC2, (c) XC3, and (d) XC4, on the carbon sequestration of a 40 MPa Type I (●), Type II (○), Type III (■), Type IV (□), Type V (▲), and White (△) cement concrete column ( $0.5 \times 0.5 \times 3$  m) after 100 years of exposure.



### 3.3. Effect of SCM type and percent replacement

Fig. 4 illustrates the anticipated percent reduction in carbon sequestration potential,  $C_m$  (kg CO<sub>2</sub>/kg cement) per type and amount of SCM. The data shown in Fig. 4 are independent of cement type and total cement content in the concrete mixtures. Expectedly, increased reductions in CO<sub>2</sub> sequestration are observed with increased weight-percent replacement of silica-rich SCMs. As previously discussed, when OPC is partially replaced by SCMs, the pozzolanic nature of siliceous SCM minerals react with CH, rendering less CH available for CO<sub>2</sub> sequestration. In addition, the reduction in CO<sub>2</sub> sequestration potential depends on the type of SCM (i.e., Class F fly ash, Class C fly ash, silica fume, slag, metakaolin). As anticipated, silica fume, the most silica-rich of all SCMs, demonstrates the greatest reduction in CO<sub>2</sub> sequestration potential, while Class C fly ash demonstrates the least reduction per weight-percent cement replacement. To achieve a 60% reduction in CO<sub>2</sub> sequestration potential, for example, would require only 10% replacement of cement with silica fume versus a 46% replacement with Class C fly ash. Class F fly ash and metakaolin demonstrate identical reductions in CO<sub>2</sub> sequestration potential due to similar silica contents on a per mass basis, which is represented by the  $\beta$  factor presented in Table 2.

The data in Fig. 4 also show upper-bound limits to pozzolanic reactivity per SCM, which coincides with an elimination of any potential for carbon sequestration. For example, if cement were replaced with silica fume, Class F fly ash (or metakaolin), slag, or Class C fly ash by more than 15%, 30%, 44%, and 60%, respectively, theoretically no CO<sub>2</sub> sequestration would be expected according to this model.

### 3.4. Effect of environmental exposure

The effect of CO<sub>2</sub> concentration (ppm), exposure classification (i.e., XC1, XC2, XC3, XC4), and cement type on the carbon sequestration of a 40 MPa concrete column (0.5 × 0.5 × 3 m) after 100 years of exposure is shown in Fig. 5. Expectedly, an increase in CO<sub>2</sub> concentration (ppm) resulted in higher *in situ* CO<sub>2</sub> sequestration for all exposure classifications and cement types. A surface-exposed column placed indoors, for example, (XC1) with a high concentration of CO<sub>2</sub> (2000 ppm) absorbs 216% more CO<sub>2</sub> after 100 years than if it were exposed to lower concentrations (200 ppm). This finding suggests that elevated levels of CO<sub>2</sub> may be beneficial to promote *in situ* CO<sub>2</sub> sequestration in an indoor environment.

Results in Fig. 5 also demonstrate the influence of exposure classification on in-service carbon sequestration potential. For example, an exposed-surface column inside a building (XC1) will absorb a higher amount of CO<sub>2</sub> than concrete columns submerged in soil or water (XC2), encased and protected from ambient conditions (XC3), or exposed to wetting/drying cycles or rain (XC4). A 40 MPa White cement concrete column in XC1 exposed to a high concentration (1000 ppm) of CO<sub>2</sub>, for example, sequesters 121% more CO<sub>2</sub> after 100 years than the same column located in XC4 at the same CO<sub>2</sub> concentration. In instances where concrete surfaces are not exposed to the surrounding environment (XC2), in-service carbon sequestration potential is reduced. The same 40 MPa White cement concrete column that is surface-exposed inside a building (XC1) to a low-CO<sub>2</sub> concentration environment (400 ppm) absorbs 372% more CO<sub>2</sub> than a column that is not exposed (XC2) at the same CO<sub>2</sub> concentration after 100 years. In summary, the data in Fig. 5 further suggest that *in situ* CO<sub>2</sub> sequestration is maximized in low-C<sub>4</sub>AF cement (Type III, V, White) concretes, as previously elucidated in Section 3.1, and in elements that are surface-exposed to high-CO<sub>2</sub> concentrations in indoor environments. Such findings can be leveraged to inform and maximize the benefit of carbon-capture and carbon-storage strategies in low-carbon building.

### 3.5. Effect of structural geometry

In recognition that carbonation and, thus, carbon sequestration of concrete elements is a surface-dominated phenomenon, Fig. 6 illustrates the effect of structural geometry, namely SA/V ratio of Type I, 40 MPa concrete columns with varying cross-sectional dimensions presented in Table 7, and length of exposure on CO<sub>2</sub> sequestration potential in both an indoor (XC1) high-concentration (800 ppm) CO<sub>2</sub> (Fig. 6a) and an outdoor (XC4) low-concentration (300 ppm) CO<sub>2</sub> (Fig. 6b) environment.

The data in both Fig. 6a and b demonstrate that higher SA/V ratios result in higher amounts of sequestered carbon at all ages of in-service exposure. For instance, a cross-shaped column section (SA/V = 15.1 m<sup>-1</sup>) will absorb 198% more CO<sub>2</sub> than a traditional cylindrical column of the same volume (SA/V = 7 m<sup>-1</sup>). Therefore, if the geometries of all 25 columns in a medium-size office building that were exposed to the interior (800 ppm) were altered to increase the SA/V ratio from 7 m<sup>-1</sup> to 15 m<sup>-1</sup>, an additional 110% (795 kg) CO<sub>2</sub> could be sequestered after 50 years. If, for example, the geometries were changed from cylindrical to swirl-shaped (SA/V = 20 m<sup>-1</sup>), after 25 years of exposure in the same high-concentration CO<sub>2</sub> environment, the 25 columns in the building

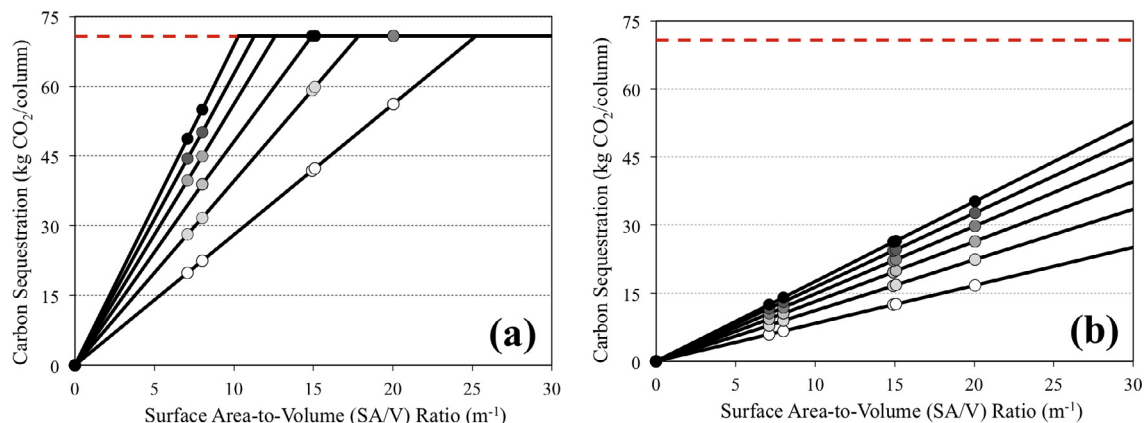


Fig. 6. Influence of SA/V ratio on sequesterable CO<sub>2</sub> for Type I, 40 MPa structural concrete columns ( $V = 0.75 \text{ m}^3$ ) in (a) high-(800 ppm) and (b) low-concentration (300 ppm) CO<sub>2</sub> environments after 25 (○), 50 (◐), 75 (◑), 100 (●), 125 (●), and 150 (●) years. Theoretical limit (—) assumes a service life,  $t = \infty$ .

could sequester 185% (910 kg) more CO<sub>2</sub>. Percent increases are identical in either a high- or low-concentration CO<sub>2</sub> environment, rendering the SA/V-related increases in carbon sequestration potential independent of environmental exposure.

Fig. 6 also illustrates that, while higher SA/V ratios result in higher amounts of sequestered carbon at all finite ages of exposure, all shapes will eventually reach the theoretical limit of 70.8 kg CO<sub>2</sub> at infinite ages for this particular volume ( $V = 0.75\text{m}^3$ ) of Type I, 40 MPa concrete. In this analysis, a 100% carbonation degree has been assumed, thus concrete elements with high SA/V ratio ( $SA/V > 15\text{ m}^{-1}$ ) located in high CO<sub>2</sub> concentration environments can reach this theoretical limit after 75–100 years. However, realistic volumes of concrete elements will not likely reach theoretical limits while in service. Practically, concrete structures would likely reach their theoretical limit post-deconstruction, when concrete elements are demolished and crushed into high surface-area rubble. In this case, concrete may experience accelerated carbonation and, depending upon post-deconstruction exposure conditions, could reach the theoretical limit prescribed by the model proposed herein. When incorporating this particular model into WBLCA, the estimated CO<sub>2</sub> sequestered will vary depending on the chosen system boundary. For instance, in a cradle-to-cradle study, where the effects of post-use crushing and recycling concrete are included, it can be immediately assumed that the volume carbonated will be equivalent to the total volume of the concrete element (i.e.,  $t = \infty$ ). However, in cases where the system boundary of interest does not include end-of-life exposure (i.e.,  $t \neq \infty$ ), the carbon sequestration benefits of post-use carbon sequestration are not included in the model prediction.

The magnitude of carbon sequestration in relation to initial carbon emissions is highly dependent upon the cradle-to-gate lifecycle assessment of the OPC concrete element. Recent studies have shown that certain concrete elements can sequester anywhere from 15 to 17% of initial CO<sub>2</sub> emissions [27] or up to 41% [26]. The results from this study indicate that the degree of recarbonation of any structural element will be highly dependent not only on the initial carbon emissions during manufacture, transport, and construction, but also on the type and amount of cement, SCMs, compressive strength, and geometry of the individual concrete element.

It is evident from the data that, for the same volume of concrete, high SA/V-ratio geometries are preferred in terms of carbon sequestration potential for structures with less than 50 years of exposure. In order to achieve higher SA/V ratios, however, complex structural shapes are required. Circular and square cross-sections, which exhibit the lowest SA/V ratios, currently dominate for fast, low-cost construction. However, more complex structural shapes could be made possible by emerging technologies, such as additive manufacturing (3D printing).

Finally, Fig. 6 illustrates that high CO<sub>2</sub> environments enhance *in situ* CO<sub>2</sub> sequestration, which, in concert with findings presented in previous sections, indicates that a combination of (1) innovations in structural geometries (high SA/V ratios), (2) high CO<sub>2</sub> exposure, (3) low-C<sub>4</sub>AF cements, (4) no SCMs, (5) low-compressive strengths at early ages, (6) high-compressive strengths at later ages, and (7) interior placement would be most favorable in order to strategically maximize the in-service CO<sub>2</sub> sequestration potential of exposed reinforced concrete elements.

#### 4. Conclusions

A simple model for predicting the carbon sequestration potential of exposed ordinary portland cement (OPC) concrete elements was formulated and implemented in this work. The model, which is based on OPC cement hydration and carbonation reaction chem-

istry, accounts for type and quantity of cements and weight-percent replacement of cement by supplementary cementitious materials (SCMs). The effects of each of these parameters on the theoretical carbon dioxide (CO<sub>2</sub>) sequestration of OPC concrete elements were investigated for a variety of CO<sub>2</sub> environmental exposure classifications. In addition, the influence of concrete design compressive strength and structural geometry, namely the effect of increasing surface-area-to-volume (SA/V) ratio of exposed concrete elements, on sequesterable CO<sub>2</sub> was investigated herein.

As anticipated, the results confirm that total sequesterable CO<sub>2</sub> increases not only with exposure time, but also with CO<sub>2</sub> concentration while in service. In addition, White cement exhibited the highest CO<sub>2</sub> sequestration potential of all cement types, due to its low C<sub>4</sub>AF content. Results also suggest that low-strength concretes sequester more CO<sub>2</sub> at early ages, but high-strength concretes sequester more CO<sub>2</sub> at later ages, elucidating a time-dependent influence of compressive strength on total carbon sequestration.

The data illustrate that, when OPC is partially replaced by SCMs, the CO<sub>2</sub> sequestration potential is reduced and that this reduction depends upon type of SCM and weight-percent cement replacement. Silica-rich SCMs, such as silica fume, Class F fly ash, and metakaolin, exhibit the most reductions in CO<sub>2</sub> sequestration potential per weight-percent replacement compared to SCMs with lower silica contents (e.g., slag, Class C fly ash). Furthermore, the amount of sequesterable CO<sub>2</sub> depends on the exposure classification of the OPC concrete element. CO<sub>2</sub> sequestration was enhanced in permanently dry or humid conditions and reduced in cyclically humid and dry conditions, suggesting that it is favorable to place OPC concrete elements inside the building envelope rather than outside to enhance *in situ* sequestration.

Innovative structural geometries, namely increasing the SA/V ratios of concrete elements, can enhance the carbon sequestration potential of OPC concrete structures. By analyzing columns of similar volumes but with varying surface-area geometries, it was found that total, *in situ* sequesterable CO<sub>2</sub> can be enhanced by up to 255% compared to round, cylindrical columns. Innovative geometries required for high-SA/V ratio structural elements are increasingly achievable with advancements in additive manufacturing construction technologies.

The model presented herein can be employed to quantify carbon sequestration potential of reinforced OPC concrete elements when implementing a whole-building lifecycle assessment (WBLCA). Total sequesterable carbon can be calculated for concrete elements while in service (assuming a finite lifetime) or out of service (assuming an infinite lifetime). As discussed, the model presented in this paper is notably conservative, since it does not account for participation by other ferritic or calcium-containing compounds (i.e., CSH) in the carbon sequestration process.

In summary, the findings suggest that novel materials design considerations (low C<sub>4</sub>AF cement, low compressive strength, no SCMs), structural concrete design innovations (high SA/V ratio), and new air quality strategies (minimum ppm CO<sub>2</sub>) could be implemented to maximize *in situ* sequestration via exposure of OPC concrete elements to CO<sub>2</sub>-rich environments. Given that enhanced carbonation during service may lead to premature serviceability concerns with carbonation-induced corrosion of mild steel reinforcement, design decisions related to maximizing carbon sequestration potential of exposed OPC concrete should be made within a more holistic lifecycle sustainability context.

#### Acknowledgments

This work was made possible by the Department of Civil, Environmental, and Architectural Engineering, the College of Engineering and Applied Sciences, and the Sustainable Infrastructure

Materials Laboratory (SIMLab) at the University of Colorado Boulder, with partial support from the National Science Foundation (Award No. CMMI-1562557). It represents views of the authors and not necessarily those of the sponsors.

## References

- [1] T. Ramesh, R. Prakash, K.K. Shukla, Life cycle energy analysis of buildings: an overview, *Energy Build.* 42 (2010) 1592–1600.
- [2] A. Haapio, P. Viitaniemi, A critical review of building environmental assessment tools, *Environ. Impact Assess. Rev.* 28 (7) (2008) 469–482.
- [3] I.Z. Bribián, A.A. Usón, S. Scarpellini, Life cycle assessment in buildings: State-of-the-art and simplified LCA methodology as a complement for building certification, *Build. Environ.* 44 (12) (2009) 2510–2520.
- [4] J. Basbagill, F. Flager, M. Lepech, M. Fischer, Application of life-cycle assessment to early stage building design for reduced embodied environmental impacts, *Build. Environ.* 60 (2013) 81–92.
- [5] S. Junnila, A. Horvath, Life-cycle environmental effects of an office building, *J. Infrastruct. Syst.* 9 (4) (2003) 157–166.
- [6] B.L.P. Peuportier, Life cycle assessment applied to the comparative evaluation of single family houses in the French context, *Energy Build.* 33 (5) (2001) 443–450.
- [7] L.F. Cabeza, L. Rincón, V. Vilarinho, G. Pérez, A. Castell, Life cycle assessment (LCA) and life cycle energy analysis (LCEA) of buildings and the building sector: a review, *Renew. Sustain. Energy Rev.* 29 (2014) 394–416.
- [8] M. Khasreen, P. Banfill, G. Menzies, Life-cycle assessment and the environmental impact of buildings: a review, *Sustainability* 1 (3) (2009) 674–701.
- [9] E. Worrell, L. Price, N. Martin, C. Hendriks, L.O. Meida, Carbon dioxide emissions from the global cement industry 1, *Annu. Rev. Energy Env.* 26 (1) (2001) 303–329.
- [10] K.-H. Yang, Y.-B. Jung, M.-S. Cho, S.-H. Tae, Effect of supplementary cementitious materials on reduction of CO<sub>2</sub> emissions from concrete, *J. Clean. Prod.* (2015) 774–783.
- [11] F.P. Torgal, S. Miraldo, J.A. Labrincha, J. De Brito, An overview on concrete carbonation in the context of eco-efficient construction: evaluation, use of SCMs and/or RAC, *Constr. Build. Mater.* (2012) 141–150.
- [12] I. Galan, C. Andrade, P. Mora, M. San Juan, Sequestration of CO<sub>2</sub> by concrete carbonation, *Environ. Sci. Technol.* 44 (8) (2010) 3181–3186.
- [13] M. Peter, A. Muntean, S. Meier, M. Bohm, Competition of several carbonation reactions in concrete: a parametric study, *Cem. Concr. Res.* 38 (12) (2008) 1385–1393.
- [14] S.K. Roy, K.B. Poh, D.O. Northwood, Durability of concrete—accelerated carbonation and weathering studies, *Build. Environ.* 34 (1999) 597–606.
- [15] W. Ashraf, Carbonation of cement-based materials: challenges and opportunities, *Constr. Build. Mater.* 120 (2016) 558–570.
- [16] S. Khashef-Haghighi, Y. Shao, S. Ghoshal, Mathematical modeling of CO<sub>2</sub> uptake by concrete during accelerated carbonation curing, *Cem. Concr. Res.* 67 (2015) 1–10.
- [17] I. Monteiro, F.A. Branco, J. De Brito, R. Neves, Statistical analysis of the carbonation coefficient in open air concrete structures, *Constr. Build. Mater.* 29 (2012) 263–269.
- [18] V.G. Papadakis, C.G. Vayenas, M.N. Fardis, Experimental investigation and mathematical modeling of the concrete carbonation problem, *Chem. Eng. Sci.* 46 (5–6) (1991) 1333–1338.
- [19] L. Jiang, B. Lin, Y. Cai, A model for predicting carbonation of high-volume fly ash concrete, *Cem. Concr. Res.* 30 (2000) 699–702.
- [20] X.-Y. Wang, H.-S. Lee, A model for predicting the carbonation depth of concrete containing low-calcium fly ash, *Constr. Build. Mater.* 23 (2) (2009) 725–733.
- [21] V.G. Papadakis, C.G. Vayenas, M.N. Fardis, Fundamental modeling and experimental investigation of concrete carbonation, *Mater. J.* 88 (4) (1991) 363–373.
- [22] A. Steffens, D. Dinkler, H. Ahrens, Modeling carbonation for corrosion risk prediction of concrete structures, *Cem. Concr. Res.* 32 (6) (2002) 935–941.
- [23] C. Pade, M. Guimaraes, The CO<sub>2</sub> uptake of concrete in a 100 year perspective, *Cem. Concr. Res.* 37 (9) (2007) 1348–1356.
- [24] F. Collins, Inclusion of carbonation during the life cycle of built and recycled concrete: Influence on their carbon footprint, *Int. J. Life Cycle Assess.* 15 (6) (2010) 549–556.
- [25] S. Lee, W. Park, H. Lee, Life cycle CO<sub>2</sub> assessment method for concrete using CO<sub>2</sub> balance and suggestion to decrease LCCO<sub>2</sub> of concrete in South-Korean apartment, *Energy Build.* 58 (2013) 93–102.
- [26] T. García-Segura, V. Yepes, J. Alcalá, Life cycle greenhouse gas emissions of blended cement concrete including carbonation and durability, *Int. J. Life Cycle Assess.* 19 (1) (2014) 3–12.
- [27] K.-H. Yang, E.-A. Seo, S.-H. Tae, Carbonation and CO<sub>2</sub> uptake of concrete, *Environ. Impact Assess. Rev.* 46 (2014) 43–52.
- [28] K. Pomer, C. Pade, Guidelines – Uptake of carbon dioxide in the life cycle inventory of concrete. Technical results from the project “CO<sub>2</sub> uptake during the concrete life cycle”, Danish Technological Institute (DTI), 2006.
- [29] B. Lagerblad, Carbon Dioxide Uptake During Concrete Life Cycle – State of the Art, Swedish Cement and Concrete Research Institute, 2006.
- [30] L.O. Nilsson, K. Fridh, CO<sub>2</sub>-cycle in cement and concrete Part 7: Models for CO<sub>2</sub>-absorption. Lund Institute of Technology, Report TVBM 7200, 2009.
- [31] T. García-Segura, V. Yepes, J.V. Martí, J. Alcalá, Optimization of concrete I-beams using a new hybrid glowworm swarm algorithm, *Latin Am. J. Solid Struct.* 11 (7) (2014).
- [32] V. Yepes, J.V. Martí, T. García-Segura, Cost and CO<sub>2</sub> emission optimization of precast-prestressed concrete U-beam road bridges by a hybrid glowworm swarm algorithm, *Autom. Constr.* 49 (A) (2015) 123–134.
- [33] American Society of Testing and Materials (ASTM), Standard specification for portland cement, West Conshohocken, PA USA, 2016.
- [34] B. Johansson, P. Utgenannt, Microstructural changes caused by carbonation of cement mortar, *Cem. Concr. Res.* 31 (6) (2001) 925–931.
- [35] T. Nishikawa, K. Suzuki, S. Ito, K. Sato, T. Takebe, Decomposition of synthesized ettringite by carbonation, *Cem. Concr. Res.* 22 (1) (1992) 6–14.
- [36] P. Mounanga, A. Khelidj, A. Loukili, V. Baroghel-Bouny, Predicting Ca(OH)<sub>2</sub> content and chemical shrinkage of hydrating cement pastes using analytical approach, *Cem. Concr. Res.* 34 (2) (2004) 255–265.
- [37] C.J. Engelsen, H. Justnes, CO<sub>2</sub> binding by concrete. A summary of the state of the art and an assessment of the total binding in by carbonation in the Norwegian concrete stock. SINTEF Building and Infrastructure, Construction Technology, Norway, 2014.
- [38] K. Fridh, B. Lagerblad, Carbonation of indoor concrete: Measurements of depths and degrees of carbonation. Lund University, Report TVBM 3169, 2013.
- [39] K. Van Balen, Carbonation reaction of lime, kinetics at ambient temperature, *Cem. Concr. Res.* 35 (4) (2005) 647–657.
- [40] M. Thiery, P. Dangla, P. Belin, G. Habert, N. Roussel, Carbonation kinetics of a bed of recycled concrete aggregates: a laboratory study on model materials, *Cem. Concr. Res.* 46 (2013) 50–65.
- [41] G. Villain, M. Thiery, Gammadensimetry: a method to determine drying and carbonation profiles in concrete, *NDT and E Int.* 39 (4) (2006) 328–337.
- [42] S.H. Kosmatka, W.C. Panarese, B. Kerkhoff, Design and Control of Concrete Mixtures, vol. 5420, Portland Cement Association, Skokie, IL, 2002.
- [43] S.N. Rudnick, D.K. Milton, Risk of indoor airborne infection transmission estimated from carbon dioxide concentration, *Indoor Air* 13 (3) (2003) 237–245.